

# Synthesis and Hollow-Sphere Nanostructures of Optically Active Metal-Free Phthalocyanine

Wei Lv,<sup>[a]</sup> Xiaomei Zhang,<sup>\*[a]</sup> Jitao Lu,<sup>[a]</sup> Yuexing Zhang,<sup>[a]</sup> Xiyu Li,<sup>[a]</sup> and Jianzhuang Jiang<sup>\*[a]</sup>

**Keywords:** Phthalocyanines / Chirality / Hollow spheres / Nanostructures / Self-assembly

Optically active metal-free phthalocyanine (**1**) decorated with four octyl chains linked through binaphthyl units to the phthalocyanine ring was designed and prepared. This compound was characterized by a wide range of spectroscopic methods in addition to elemental analysis. By employing a solution injection method, both the (*R*) and (*S*) enantiomers self-assemble into nanoparticles. Surprisingly, with the addition of a small amount of cetyltrimethylammonium bromide (CTAB), nanostructures with hollow-sphere morphologies were formed. The hollow-spherical structure was determined by transmission electronic microscopy and scanning electronic microscopy. X-ray photoelectron spectroscopy together with FTIR spectra indicates the supramolecular structures

formed from the metal-free phthalocyanine molecules. Low-angle X-ray diffraction reveals the stacked phthalocyanine molecules with a face-to-face configuration in the nanoscale hollow spheres formed with the help of CTAB surfactant. The formation of *H*-aggregates in the nanoscale hollow spheres is further confirmed by electronic absorption spectroscopic result. This work, representing the first example of controllable organic nanostructures with a hollow sphere morphology fabricated from phthalocyanine provides an effective method towards phthalocyanine hollow nanospheres.

(© Wiley-VCH Verlag GmbH & Co. KGaA, 69451 Weinheim, Germany, 2008)

## Introduction

The controlled organization of functional dyes into highly ordered self-assembled array is of great interest in chemistry and nanotechnology, and it is expected to yield new materials that exhibit peculiar and fascinating photo-physical and (opto)electronic properties superior to their bulk counterparts as a result of excitonic interaction between adjacent dye molecular units.<sup>[1]</sup> Spontaneous self-assembly of molecules into supramolecular structures depends mainly on noncovalent interactions including hydrogen bonding, electrostatic, dipole–dipole, and van der Waals interactions. A variety of artificial self-assembled nanostructures with the morphology of fibers,<sup>[2]</sup> ribbons,<sup>[3]</sup> particles,<sup>[4]</sup> tubes,<sup>[5]</sup> and vesicles<sup>[6]</sup> have been prepared from different molecular materials. Among which, hollow spheres represent an appealing class of nanostructures due to their many potential applications in drug delivery, chemical storage, light filters, chemical catalysis, and as templates for preparing functional architectural composite materials.<sup>[7]</sup> As a consequence, great effort has been paid to fabricate inorganic and organic nanostructures with hollow-sphere morphologies.<sup>[8,9]</sup> The common methods used to

prepare inorganic hollow spheres include sacrificial template or interfacial synthesis. A necessary step for these methods involves the removal of the template, resulting in complication of the preparation procedure. In contrast, organic hollow spheres are usually easily prepared from the self-assembly of amphiphilic molecules through the utilization of two immiscible liquid phases. In addition, several new techniques such as sonochemical<sup>[10]</sup> and solvothermal methods<sup>[11]</sup> have also been developed to prepare organic hollow nanospheres.

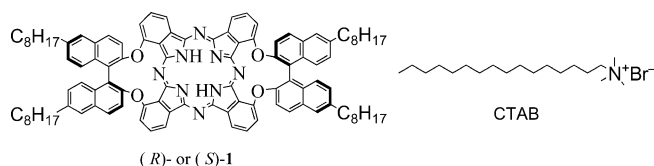
Phthalocyanine compounds, the structural analogues of porphyrins, have been intensively studied due to their high stability and useful catalytic, chemical-sensing, and optical-limiting properties.<sup>[12]</sup> Thus far, various self-assembled nanostructures, in particular nanofibers and nanotubes, have been synthesized from phthalocyanine derivatives depending on the strong  $\pi$ – $\pi$  interaction between the adjacent molecules.<sup>[13]</sup> For the purpose of preparing nanoscale hollow spheres from phthalocyanine compounds, great effort has been paid to change the nature of the phthalocyanine molecules, from hydrophobic to amphiphilic, by introducing hydrophilic substituents onto the peripheral positions of the phthalocyanine ring.<sup>[14]</sup> However, to the best of our knowledge, nanoscale hollow spheres fabricated from phthalocyanine derivatives have not yet been reported thus far. Actually, self-assembled nanostructures with hollow sphere morphologies from porphyrin compounds are also very scarce and limited to the reports of Aida<sup>[15]</sup> and Li.<sup>[6b]</sup>

[a] Department of Chemistry, Shandong University  
Jinan 250100, China  
Fax: +86-531-856-5211  
E-mail: jzjiang@sdu.edu.cn

Supporting information for this article is available on the WWW under <http://www.eurjic.org> or from the author.

It appears that adjusting the balance of the  $\pi$  stacking and van der Waals interactions between the phthalocyanine molecules cannot be easily reached by only regulating the single molecular structure. As a result, surfactant molecules have been employed to introduce the hydrophilic properties into the hydrophobic molecules by means of hydrophobic interactions between the dye and the surfactant molecules. CTAB (cetyltrimethylammonium bromide) has been among one of the widely utilized surfactants to coassemble with some dye molecules.<sup>[16]</sup> For example, Wan and coworkers fabricated ZnTPyP into nanotubes by using CTAB as an additive.<sup>[5c]</sup> However, there has been no report on nanostructures with a hollow-spherical morphology fabricated from phthalocyanine derivatives with the help of surfactant additives.

In this paper, the self-assembly properties of a novel optically active metal-free phthalocyanine compound (**1**) decorated with four octyl chains linked through binaphthyl units to the phthalocyanine ring has been comparatively studied with and without the addition of CTAB surfactant (Scheme 1) after molecular design, synthesis, and characterization. According to theoretical calculations, introduction of the two bulky binaphthyl units onto the nonperipheral positions of the phthalocyanine ring not only induces optical activity onto the phthalocyanine ligand but also diminishes the  $\pi$ - $\pi$  interaction between adjacent phthalocyanine molecules due to steric hindrance.<sup>[17]</sup> Meanwhile, incorporation of the four octyl chains onto the two binaphthyl units leads to an increase in the hydrophobic interaction between the molecules of metal-free phthalocyanine (**1**) and the CTAB molecules. As a consequence, the molecules of this metal-free phthalocyanine compound self-assemble into nanoparticles. In good contrast, with the assistance of CTAB, nanoscale hollow spheres are fabricated from this metal-free phthalocyanine compound. The present work, representing the first example of controllable organic nanostructures fabricated from phthalocyanine compound, provides an effective method towards phthalocyanine nanostructures with a hollow-sphere morphology.

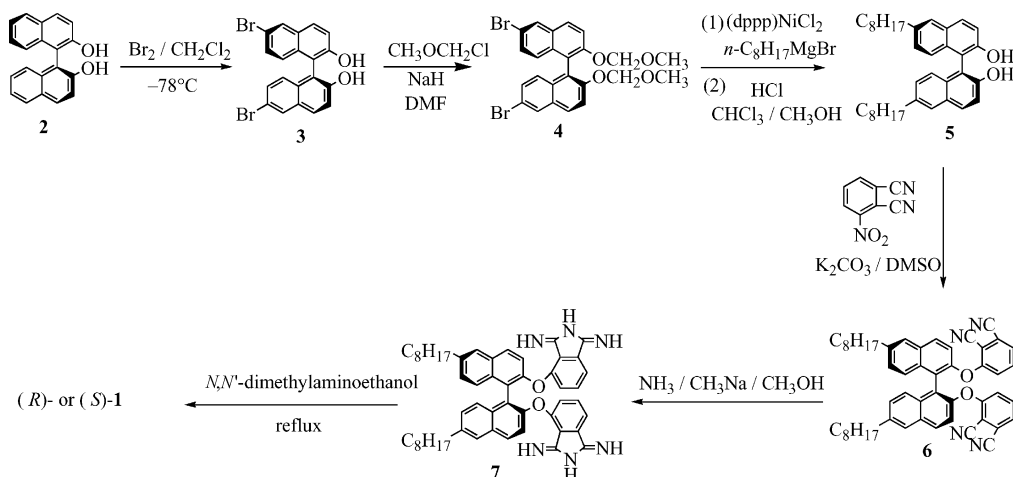


Scheme 1. Schematic molecular structure of (*R*)- or (*S*)-**1** and CTAB.

## Results and Discussion

### Synthesis

Despite the huge number of various kinds of substituted phthalocyanine compounds reported thus far, examples of optically active phthalocyanines with low molecular symmetry still remains rare. In the present study, the optically active metal-free phthalocyanine **1** was prepared from (*R*)- or (*S*)-diiminoisoindoline derivative (**7**). As shown in Scheme 2, binaphthylol derivative **6** was obtained from a nucleophilic aromatic substitution reaction between 3-nitrophenol and (*R*)- or (*S*)-2,2'-dihydroxy-6,6'-dioctyl-1,1'-binaphthyl (**5**), which was prepared from a protection reaction, Grignard reaction, and deprotection reaction of (*R*)- or (*S*)-2,2'-dihydroxy-6,6'-dibromo-1,1'-binaphthyl (**3**). By bubbling ammonia gas into a dry methanol solution, binaphthylol derivative **6** was converted into diiminoisoindoline derivative **7**. Cyclic tetramerization of **7** in refluxing (*N,N*-dimethylamino)ethanol provided the target optically active metal-free phthalocyanine compound (*R*)-**1** and (*S*)-**1**. Satisfactory elemental analysis was obtained for this newly prepared optically active phthalocyanine compound after repeated column chromatography and recrystallization. This compound was also characterized by <sup>1</sup>H NMR spectroscopy (Figure S1, Supporting Information), electronic absorption, IR spectroscopy, and



Scheme 2. The synthesis of optically active (*R*)- or (*S*)-**1**.

MALDI-TOF (Figure S2, Supporting Information) mass spectrometry. The optical purity of the compound at each reaction step was examined either by comparative experiments or by confirming that the recovered unreacted optically active material had very little or no rotational loss.

### Electronic Absorption and Circular Dichroism Spectroscopy

Figure 1 shows the electronic absorption spectrum and circular dichroism spectra of metal-free phthalocyanine (*R*)-**1** and (*S*)-**1** in chloroform. In the spectrum, the phthalocyanine Soret band appears at 339 nm. In particular, this metal-free phthalocyanine exhibits typical characteristic split for Q-bands for nonaggregated metal-free phthalocyanine with the maxima appearing at 659 and 692 nm, respectively. In addition, the intense absorption below 270 nm is attributed to the absorption of binaphthyl groups, which is supported by the corresponding CD signals for (*R*)-**1** and (*S*)-**1** in their CD spectra. It can be seen from the CD spectra that introduction of the optically active binaphthyl moieties onto the periphery of the phthalocyanine ring induces the appearance of CD signals of phthalocyanine compound in both the Soret and Q absorption regions (Figure 1). In the case of (*S*)-**1**, the sign of the CD is mainly negative over the main Soret and Q bands. Conversely, (*R*)-**1** shows mainly a positive CD sign. According to the chiral exciton theory,<sup>[18]</sup> (*S*)-**1** is right-handed, whereas (*R*)-**1** is left-handed on the basis of the CD pattern in the 220–270 nm region.

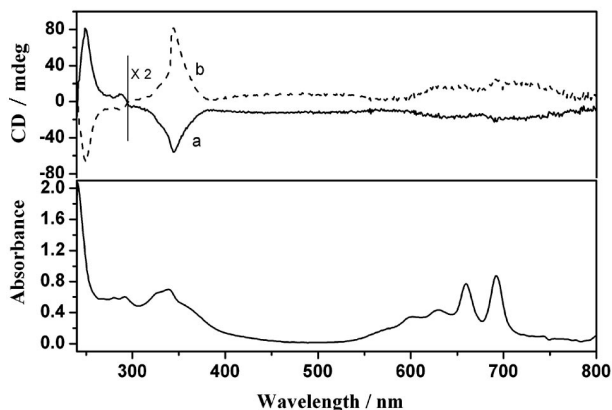


Figure 1. Circular dichroism of (*S*)-**1** (a) and (*R*)-**1** (b) together with the electronic absorption spectrum in chloroform.

Figure S3 (Supporting Information) displays the electronic absorption spectrum of metal-free phthalocyanine (**1**) in chloroform as well as those in mixed solvent of chloroform and methanol. As can be found, along with the addition of methanol, both the Soret and Q bands gradually lose their intensity. In particular, the two main Q bands gradually shift to the higher energy side. When the ratio of chloroform and methanol reaches 1:9, well-defined Q bands of **1** at 65 and 692 nm disappear and a very broad band

with a maximum at 627 nm is observed. These results indicate the formation of *H*-type aggregates of **1** in chloroform with the addition of methanol,<sup>[19]</sup> revealing the face-to-face molecular arrangement in the nanoparticles formed. The electronic absorption spectra of **1** in chloroform and mixed solution of chloroform and methanol with the addition of CTAB are compared in Figure 2. Actually, by increasing the methanol content, **1** with the help of CTAB surfactant also experiences a similar blueshift in its Q absorption bands and an intensity decrease in both the Soret and Q bands. Finally, a broadened Q band with a maximum at 632 nm is observed when the ratio of chloroform and methanol reaches 1:9.

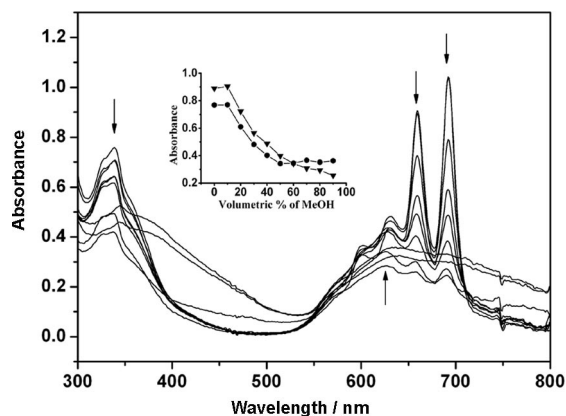


Figure 2. Electronic absorption spectra of metal-free phthalocyanine **1** with the addition of CTAB in chloroform/methanol in the ratio of 10:0, 9:1, 8:2, 7:3, 6:4, 5:5, 4:6, 3:7, 2:8, and 1:9. The inset shows the absorbance change in the Q-bands of **1** before (●) and after (▼) the addition of CTAB.

The inset of Figure 2 shows the absorbance change of the Q band for **1** at 692 nm before and after the addition of CTAB. As can be seen, in pure chloroform, this Q band remains almost unchanged in terms of energy but slightly increases in the absorption intensity after the addition of CTAB. With an increase in solvent polarity (without adding CTAB), the intensity of this Q absorption gradually decreases and reaches a constant value in mixed solvent containing more than 50% methanol. In contrast, in the presence of CTAB, the intensity of this Q band continuously decreases even after the ratio of methanol and chloroform is greater than 1:1. These results indicate the aggregation properties of **1** in solution were influenced with the addition of CTAB.<sup>[13c]</sup>

### Aggregate Morphology

The morphology of the aggregates was examined by scanning electron microscopy (SEM) and transmission electron microscopy (TEM). Samples were prepared by casting a drop of sample solution onto a carbon-coated grid. Both aggregated images obtained from the solution with and

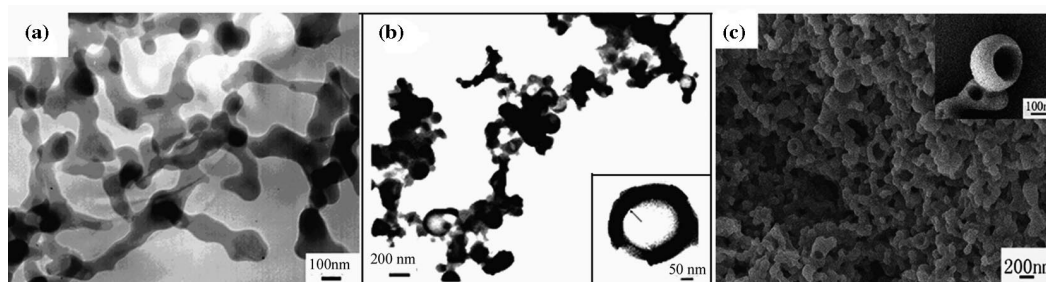


Figure 3. (a) TEM image of metal-free phthalocyanine nanoparticles; (b) TEM image of nanoscale hollow spheres, and the inset is a high-magnification TEM image showing the hollow structure; (c) SEM image of nanoscale hollow spheres, and the inset is a high-magnification SEM image showing the broken structure.

without CTAB are shown in Figure 3. Before the addition of surfactant (Figure 3a), large-scale nanoparticles with an average particle radius of 100–150 nm were fabricated. However, when aggregates were formed with the help of the CTAB surfactant, nanoparticles with the presence of circular rings of a sectioned sphere and a bright cavity in the interior were formed (Figure 3b). In contrast to the image of the entirely dark spherical nanostructures obtained without the addition of CTAB, the visual insights into the inner-hollow nanostructures obtained by coassembly of metal-free phthalocyanine and CTAB were clearly proved. The average diameter of these hollow nanospheres is about 200 nm. The high-magnification TEM image in the inset of Figure 3b shows that the thickness of these hollow spheres is about 50 nm. Further evidence to confirm the hollow-sphere nanostructures comes from the SEM image shown in Figure 3c. As can be seen, well-defined spherical structures have been prepared, most of which remain intact. Only a few appear to be deformed or cracked. In particular, the hollow structure of the nanospheres is clearly revealed from a typical broken spherical image shown in the inset of Figure 3c.

### Assembly Mechanism

On the basis of the above-described experimental results, the formation mechanism was thus proposed as shown in Figure 4a–c. It is well known that in selective solvents, amphiphilic molecules like liposomes form micelles that would normally belong to the super-strong segregation limit (SSSL) mainly owing to the different solubility of the hydrophilic and hydrophobic units.<sup>[20]</sup> When the molecules of **1** begin to aggregate without the addition of CTAB, the bulk binaphthyl units attached onto the nonperipheral positions of the phthalocyanine ring prevent effective stacking of the phthalocyanine molecules, resulting in the formation of nanoparticles.<sup>[21]</sup> With the addition of CTAB, the interactions between CTAB and the metal-free phthalocyanine molecules not only induces the formation of the amphiphilic complexes but also improves the  $\pi$ - $\pi$  stacking between the phthalocyanine molecules as proved by the electronic absorption spectroscopic result (vide supra), finally

resulting in the formation of nanoscale hollow spheres. This is supported by the results of X-ray photoelectron spectroscopy (XPS) on the composition of phthalocyanine nanoscale hollow spheres obtained with the help of the CTAB surfactant.

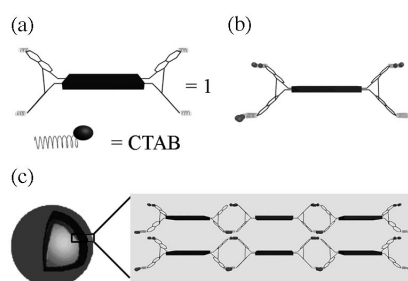


Figure 4. (a) Schematic representation of **1** and CTAB; (b) schematic representation of the interaction between **1** and the CTAB molecules; (c) schematic illustration of a hollow sphere formed in methanol with a close up of the membrane showing the proposed structure.

### XPS Analysis

In order to obtain further information on the outer surface of the hollow-spherical aggregates, X-ray photoelectron spectroscopy (XPS) was used to detect their elemental composition. As shown in Figure 5a, the peaks located at 154 and 534 eV are attributed to Br (2p) and O (1s), respectively. In particular, the signal due to the 1s band of the nitrogen element is found to split into two peaks at 399.1 and 400.5 eV (Figure 5b), revealing the two different chemical states of the nitrogen atoms in the hollow nanospheres from the phthalocyanine and CTAB moieties.<sup>[22]</sup> As a result, observation of the elemental signature for the N, O, and Br atoms in the XPS spectrum confirms the composition of the nanoscale hollow spheres from metal-free phthalocyanine **1** with the help of CTAB.

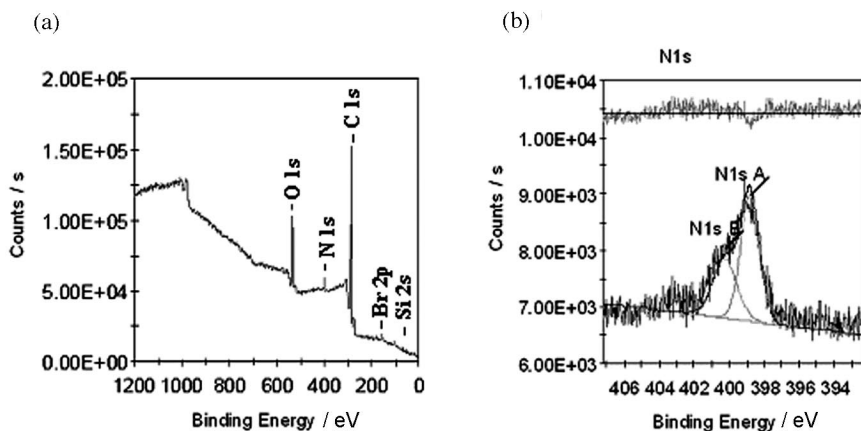


Figure 5. (a) XPS spectrum of hollow spherical aggregates formed from metal-free phthalocyanine **1** with the help of CTAB; (b) XPS spectrum of nitrogen element indicating the two different chemical states in the hollow spherical aggregates.

### XRD Analysis

The structures of the nano self-assemblies were further investigated by low-angle X-ray diffraction (XRD) technique. Figure 6a shows the diffraction pattern of the two self-assembled nanostructures. As can be seen, there exists no diffraction peak in the X-ray diffraction pattern of the nanoparticles self-assembled from **1**, which indicates the lack of ordered molecular packing in this nanostructure due to the lack of effective intermolecular  $\pi$ - $\pi$  interactions. In contrast, two sharp diffraction peaks appear in the X-ray diffraction pattern of the hollow spheres at  $2\theta = 3.33$  and  $6.72^\circ$ , indicating the regularity of the molecular stacking. This diffraction pattern could be due to the refraction from the lamellar structure of the hollow spherical shell. The  $d$  spacings calculated according to these results are 2.67 and 1.31 nm, respectively. According to the geometry optimization of **1**, the height of the molecule is about 1.02 nm (Figure 6b). Considering the average stacking distance between neighboring phthalocyanine rings (0.34 nm) obtained on the basis of single-crystal X-ray diffraction analysis,<sup>[23]</sup> the sharp peak observed at 1.31 nm in the nanoscale hollow spheres can therefore be assigned to the height of one layer of the lamellar structure and that at 2.67 nm represents the distance of two layers (Figure 6b). These results indicate

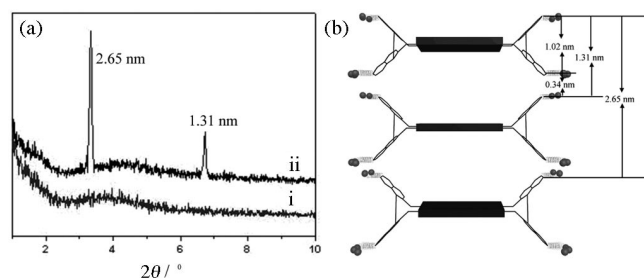


Figure 6. (a) XRD profile of the metal-free phthalocyanine nanoparticles (i) and hollow spheres of **1** formed with the addition of CTAB (ii); (b) the right side shows the schematic representation of trimer **1** with CTAB.

that the phthalocyanine molecules form ordered *H*-aggregates in the membrane of the hollow nanospheres with the help of the CTAB surfactant.

### FTIR Spectra

The FTIR spectra of **1**, the nanoparticles, the nanoscale hollow spheres, and CTAB are compared in Figure S4 (Supporting Information). The similar features, except for the decreased intensity in the IR spectra of both the nanoparticles and the nanoscale hollow spheres, to that of **1** unambiguously confirms the composition of the nanoparticles and the nanoscale hollow spheres from metal-free phthalocyanine **1**. It is worth noting that the intense band observed at approximately  $1397\text{ cm}^{-1}$  for the ammonium ion vibration of CTAB shifts to  $1385\text{ cm}^{-1}$  as a weak band in the nanoscale hollow spheres, which reveals the effective interaction between metal-free phthalocyanine **1** and the CTAB molecules.

### Conclusions

In summary, novel optically active metal-free phthalocyanine with low molecular symmetry decorated with four octyl chains linked through binaphthyl units to the phthalocyanine ring has been designed, synthesized, and successfully fabricated into nanoscale hollow spheres with the help of surfactant through an effective and facile method. This represents the first example of nanoscale hollow spheres self-assembled from phthalocyanine derivatives. Owing to the high chemical and thermal stability of phthalocyanine compounds, the hollow spheres obtained are expected to have applications in advanced functional materials.

### Experimental Section

**Measurements:**  $^1\text{H}$  NMR spectra were recorded with a Bruker DPX 300 spectrometer (300 MHz) in  $\text{CDCl}_3$  by using the residual solvent

resonance of  $\text{CHCl}_3$  at  $\delta = 7.26$  ppm relative to  $\text{SiMe}_4$  as an internal reference. MALDI-TOF mass spectra were detected with a Bruker BIFLEX III ultra-high resolution Fourier transform ion cyclotron resonance (FT-ICR) mass spectrometer with  $\alpha$ -cyano-4-hydroxycinnamic acid as matrix. Electronic absorption spectra were obtained with a Hitachi U-4100 spectrophotometer. Elemental analyses were performed by the Department of Chemistry, Shandong University. Fourier transform infrared spectra were recorded in KBr pellets with  $2\text{ cm}^{-1}$  resolution by using a  $\alpha$ ALPHA-T spectrometer. Transmission electron microscopic images were measured with a JEOL-100CX II electron microscope operating at 100 KV. Scanning electron microscopic images were obtained with a JEOL JSM-6700F. Circular Dichroism (CD) measurements were carried out with a JASCO J-810 spectropolarimeter. X-ray photoelectron spectroscopy was performed with a ESCALAB 250I-XL photoelectron spectrometer by using  $\text{Al-K}\alpha$  as the exciting source. For TEM imaging, a drop of the sample solution was cast onto a carbon copper grid. For SEM imaging, Au (1–2 nm) was sputtered onto these grids to prevent charging effect and improve the image clarity. Low-angle X-ray diffraction (XRD) measurements were carried out with a Rigaku D/max-cB X-ray diffractometer.

**Chemicals:** (*N,N*-Dimethylamino)ethanol and DMF were freshly distilled just before use. Ether was freshly distilled after refluxing with metal sodium under an atmosphere of nitrogen. Both chloroform and methanol (HPLC grade) were purchased from Tianjin Kermel Co. Column chromatography was carried out on silica gel (Merck, Kieselgel 60, 70–230 mesh) with the indicated eluents. (*R*- and (*S*)-2,2'-dihydroxy-1,1'-binaphthyl (>99% ee) were purchased from Dalian Reagent Company. All the other chemicals were of reagent grade and used as received without further purification. The compounds (*R*- and (*S*)-1,1'-binaphthalene-2,2'-diol (**2**)<sup>[24]</sup> and (*R*- or (*S*)-6,6'-dibromo-1,1'-binaphthalene-2,2'-diol (**3**)<sup>[25]</sup> were prepared according to published procedures.

The optically active metal-free phthalocyanine with CTAB complex was prepared by mixing metal-free phthalocyanine **1** (4.58 mg) and CTAB (6.56 mg) together in a chloroform (10 mL) solution. The mixture was stirred for enough time to ensure homogeneity. The nanoscale hollow spheres were fabricated by solution mixed method: A methanol solution was injected into a solution of metal-free phthalocyanine with CTAB mixture in chloroform to give a final chloroform/methanol ratio of 1:2 (v/v) at 45 °C. After the solution was allowed to equilibrate over 30 min, one drop of the solution was cast onto a grid (Cu with a carbon film). The aggregated behavior was observed after the solvent was evaporated. The nanoparticles were prepared by the same method without adding CTAB. The experimental results were reproducible under the experimental conditions described above.

**(*R*- or (*S*)-6,6'-Dioctyl-1,1'-binaphthalene-2,2'-diol (**5**):** Magnesium (880 mg, 36.7 mmol) in dry ether (15 mL) was added into a three-necked flask equipped with a reflux condenser. After the vessel was flushed with nitrogen, 1-bromooctane (5.79 g, 30 mmol) in diethyl ether (20 mL) was added slowly, and the mixture was maintained at reflux. The mixture was stirred under a nitrogen atmosphere for another 3 h and then cooled to room temperature for the following reaction. To a suspension of (*R*- or (*S*)-6,6'-dibromo-2,2'-bis(methoxymethoxy)-1,1'-binaphthalene (**4**) (5.32 mg, 10 mmol) and (dppp)NiCl<sub>2</sub> (54.2 mg, 0.1 mmol) in dry ether (100 mL) was slowly added the prepared octylmagnesium bromide. Upon the addition of  $\text{C}_8\text{H}_{17}\text{MgBr}$ , the suspension turned into a clear brown solution. The reaction mixture was stirred at room temperature for 30 min and then heated at reflux for 40 h under a nitrogen atmosphere. The mixture was cooled to 0 °C and quenched with water (20 mL)

and hydrogen chloride solution (2 N, 40 mL). The aqueous layer was repeatedly extracted with diethyl ether, and the combined organic layer was washed with water and concentrated under reduced pressure. The residue was redissolved into a mixed solution of chloroform (60 mL), methanol (60 mL), and concentrated hydrogen chloride (4 mL). The reaction mixture was stirred at room temperature for 10 h and repeatedly extracted with chloroform. The combined organic layer was washed with water and dried with anhydrous  $\text{Na}_2\text{SO}_4$  and evaporated, giving the crude product. The crude product was subjected to column chromatography over silica gel [ethyl acetate/petroleum ether (60–90 °C), 1:18 v/v], giving target compound **5** (3.8 g) as liquid (61% yield). <sup>1</sup>H NMR (300 MHz,  $\text{CDCl}_3$ ):  $\delta = 0.80$ – $1.68$  (m, 30 H), 2.72 (t,  $J = 7.7$  Hz, 4 H), 5.03 (s, 2 H), 7.07 (d,  $J = 8.4$  Hz, 2 H), 7.14 (d,  $J = 9$  Hz, 2 H), 7.31 (d,  $J = 9$  Hz, 2 H), 7.63 (s, 2 H), 7.85 (d,  $J = 9$  Hz, 2 H) ppm. MS: calcd. for  $\text{C}_{36}\text{H}_{46}\text{O}_2$  [ $\text{M} + \text{H}$ ]<sup>+</sup> 511.81; found 510.81.

**(*R*- or (*S*)-2,2'-Bis(2,3-dicyanophenyl)-6,6'-dioctyl-1,1'-binaphthalene (**6**):** Potassium carbonate (2.04 g, 14.8 mmol), 3-nitrophthalonitrile (1.4 g, 8.1 mmol), and compound **5** in dry DMSO (15 mL) were stirred at room temperature under a nitrogen atmosphere for 72 h. The reaction mixture was poured into ice water (100 mL), and the aqueous layer was extracted with ethyl acetate. After being dried with anhydrous  $\text{MgSO}_4$ , the organic layer was evaporated, and the residue was purified by silica gel chromatography [ethyl acetate/petroleum ether (60–90 °C), 1:2 v/v], giving product **6** as a yellowish solid (40.6% yield). <sup>1</sup>H NMR (300 MHz,  $\text{CDCl}_3$ ):  $\delta = 0.86$  (t,  $J = 6.3$  Hz, 6 H), 1.26–1.31 (m, 20 H), 1.64 (t,  $J = 3.5$  Hz, 4 H), 2.71 (t,  $J = 7.7$  Hz, 4 H), 7.14 (d,  $J = 8.7$  Hz, 2 H), 7.22 (br., 3 H), 7.24 (br., 3 H), 7.32 (d,  $J = 8.7$  Hz, 2 H), 7.49 (t,  $J = 8.1$  Hz, 2 H), 7.68 (s, 2 H), 7.94 (d,  $J = 9$  Hz, 2 H) ppm. [ $\alpha$ ]<sub>D</sub><sup>20</sup> =  $-46.9$  ( $c = 0.8$ ,  $\text{CHCl}_3$ ) and [ $\alpha$ ]<sub>D</sub><sup>20</sup> =  $+46.7$  ( $c = 0.8$ ,  $\text{CHCl}_3$ ) for (*S*)-**6** and (*R*)-**6**, respectively.

**Diiminoisoindoline Derivative 7:** Compound **6** (1.7 g, 2.24 mmol) and sodium methoxide (121 mg, 2.24 mmol) were placed in a three-necked flask equipped with a gas inlet and refluxing condenser. The flask was flushed with anhydrous ammonia and methanol (50 mL) was added. The mixture was stirred at room temperature for 1 h and then heated at reflux for 3 h. During this period, a stream of anhydrous ammonia was slowly bubbled through the solution. After cooling, the solvent was evaporated, and the residue of **7** was used for the following reaction without further purification.

**Preparation of Metal-Free Phthalocyanine (*R*- or (*S*)-1:** Derivative **7** and (*N,N*-dimethylamino)ethanol (5 mL) were placed in a dry vessel. After the vessel was flushed with nitrogen, the mixture was stirred and heated at reflux under a nitrogen atmosphere for 3 h. After being cooled, the solvent was removed under reduced pressure. The residue was separated by chromatography (silica gel, chloroform). The first blue fraction contained (*R*- or (*S*)-**1**. The compound was recrystallized twice from chloroform and methanol. Yield: 311 mg (17%), blue solid. <sup>1</sup>H NMR (300 MHz,  $\text{CDCl}_3$ ):  $\delta = -4.54$  (s, 2 H), 0.78–0.85 (m, 12 H), 1.16–1.56 (m, 44 H), 1.99 (s, 4 H), 2.58 (s, 4 H), 3.07 (s, 4 H), 6.21 (s, 2 H), 6.47 (d,  $J = 8.4$  Hz, 2 H), 7.15–7.30 (m, 8 H), 7.45 (s, 2 H), 7.62–7.75 (m, 4 H), 7.89–8.06 (m, 6 H), 8.23 (s, 2 H), 8.69–8.83 (m, 6 H) ppm. MS: calcd. for  $\text{C}_{104}\text{H}_{102}\text{N}_8\text{O}_4$  [ $\text{M} + \text{H}$ ]<sup>+</sup> 1528.9; found 1527.9.  $\text{C}_{104}\text{H}_{102}\text{N}_8\text{O}_4 \cdot 3\text{C}_6\text{H}_{14}$ : calcd. C 82.02, H 8.12, N 6.27; found C 82.56, H 7.33, N 6.59.

**Supporting Information** (see footnote on the first page of this article): Selected spectroscopic data.

## Acknowledgments

Financial support from the Natural Science Foundation of China, Ministry of Education of China, Shandong Province, and Shandong University is gratefully acknowledged. We are also grateful to the Shandong Province High Performance Computing Centre for providing us with computer time.

- [1] a) Y. Xia, P. Yang, Y. Sun, Y. Wu, B. Mayers, B. Gates, Y. Yin, F. Kim, H. Yan, *Adv. Mater.* **2003**, *15*, 353–389; b) V. Percec, C.-H. Ahn, G. Ungar, D. J. P. Yearley, M. Möller, S. S. Sheiko, *Nature* **1998**, *391*, 161–164.
- [2] a) M. Yun, N. V. Myung, R. P. Vasquez, C. Lee, E. Menke, R. M. Penner, *Nano Lett.* **2004**, *4*, 419–422; b) H. Gan, H. Liu, Y. Li, Q. Zhao, Y. Li, S. Wang, T. Jiu, N. Wang, X. He, D. Yu, D. Zhu, *J. Am. Chem. Soc.* **2005**, *127*, 12452–12453.
- [3] a) K. Balakrishnan, A. Datar, R. Oitker, H. Chen, J. Zuo, L. Zang, *J. Am. Chem. Soc.* **2005**, *127*, 10496–10497; b) K. Balakrishnan, A. Datar, T. Naddo, J. Huang, R. Oiker, M. Yen, J. Zhao, L. Zang, *J. Am. Chem. Soc.* **2006**, *128*, 7390–7398.
- [4] X. Gong, T. Milic, C. Xu, J. D. Batteas, C. M. Drain, *J. Am. Chem. Soc.* **2002**, *124*, 14290–14291.
- [5] a) J. M. Schnur, *Science* **1993**, *262*, 1669–1676; b) T. Shimizu, M. Masuda, H. Minamikawa, *Chem. Rev.* **2005**, *105*, 1401–1444; c) J. Hu, Y. Guo, H. Liang, L. Wan, L. Jiang, *J. Am. Chem. Soc.* **2005**, *127*, 17090–17095; d) M. Steinhart, R. B. Wehrspohn, U. Gösele, J. H. Wendorff, *Angew. Chem. Int. Ed.* **2004**, *43*, 1334–1344; e) Q. Liu, Y. Li, H. Liu, Y. Chen, X. Wang, Y. Zhang, X. Li, J. Jiang, *J. Phys. Chem. C* **2007**, *111*, 7298–7301.
- [6] a) D. M. Vriezema, J. Hoogboom, K. Velonia, K. Takazawa, P. C. M. Christianen, J. C. Maan, A. E. Rowan, R. J. M. Nolte, *Angew. Chem. Int. Ed.* **2003**, *42*, 772–776; b) Y. Li, X. Li, H. Liu, S. Wang, H. Gan, J. Li, N. Wang, X. He, D. Zhu, *Angew. Chem. Int. Ed.* **2006**, *45*, 3639–3643.
- [7] a) F. Caruso, *Adv. Mater.* **2001**, *13*, 11–22; b) Y. R. Ma, L. M. Qi, J. M. Ma, H. M. Cheng, *Langmuir* **2003**, *19*, 4040–4042; c) T. Nakashima, N. Kimizuka, *J. Am. Chem. Soc.* **2003**, *125*, 6386–6387; d) F. Caruso, A. R. Caruso, H. Möhwald, *Science* **1998**, *282*, 1111–1114.
- [8] a) J. Hu, Y. Guo, H. Liang, L. Wan, C. Bai, Y. Wang, *J. Phys. Chem. B* **2004**, *108*, 9734–9738; b) D. A. Dhas, K. S. Suchck, *J. Am. Chem. Soc.* **2005**, *127*, 2368–2369; c) V. S. Murthy, J. N. Cha, G. D. Stucky, M. S. Wong, *J. Am. Chem. Soc.* **2004**, *126*, 5292–5299; d) M. S. Wong, J. N. Cha, K. S. Choi, T. J. Deming, G. D. Stucky, *Nano Lett.* **2002**, *2*, 583–587.
- [9] a) S. A. Jenekhe, X. L. Chen, *Science* **1999**, *283*, 372–375; b) H. K. Lee, K. M. Park, Y. J. Jeon, D. Kim, D. H. Oh, H. S. Kim, C. K. Park, K. Kim, *J. Am. Chem. Soc.* **2005**, *127*, 5006–5007; c) D. M. Vriezema, J. Hoogboom, K. Velonia, K. Takazawa, P. C. M. Christianen, J. C. Maan, A. E. Rowan, R. J. M. Nolte, *Angew. Chem. Int. Ed.* **2003**, *42*, 772–776; d) B. Hu, X. Jiang, Y. Ding, Q. Chen, C. Yang, *Adv. Mater.* **2004**, *16*, 933–937.
- [10] N. A. Dhas, K. S. Suslick, *J. Am. Chem. Soc.* **2005**, *127*, 2368–2369.
- [11] a) J. Zhu, S. Xu, H. Wang, J. Zhu, H. Chen, *Adv. Mater.* **2003**, *15*, 156–159; b) Q. Peng, Y. Dong, Y. Li, *Angew. Chem. Int. Ed.* **2003**, *42*, 3027–3030.
- [12] a) A. B. P. Lever, C. C. Leznoff, *Phthalocyanine: Properties and Applications*, VCH, New York, **1989–1996**, vols. 1–4; b) N. B. McKeown, *Phthalocyanines Materials: Synthesis Structure and Function*, Cambridge University Press, New York, **1998**; c) K. M. Kadish, K. M. Smith, R. Guilard, *The Porphyrin Handbook*, Academic Press, San Diego, **2000–2003**, vols. 1–20.
- [13] a) M. Kimura, H. Narikawa, K. Ohta, K. Hanabusa, H. Shirai, N. Kobayashi, *Chem. Mater.* **2002**, *14*, 2711–2717; b) K. Adachi, K. Chayama, H. Watarai, *Langmuir* **2006**, *22*, 1630–1639; c) M. Kimura, T. Muto, H. Takimoto, K. Wada, K. Ohta, K. Hanabusa, H. Shirai, N. Kobayashi, *Langmuir* **2000**, *16*, 2078–2082; d) D. M. Guldi, A. Gouloumis, P. Vázquez, T. Torres, V. Georgakilas, M. Prato, *J. Am. Chem. Soc.* **2005**, *127*, 5811–5813; e) D. Qian, T. Wakayama, C. Nakamura, J. Miyake, *J. Phys. Chem. B* **2003**, *107*, 3333–3335.
- [14] a) H. Engelkamp, S. Middelbeek, R. J. M. Nolte, *Science* **1999**, *284*, 785–788; b) C. F. V. Nostrum, S. J. Picken, A. J. Schouten, R. J. M. Nolte, *J. Am. Chem. Soc.* **1995**, *117*, 9957–9965; c) M. Kimura, K. Wada, K. Hanabusa, H. Shirai, N. Kobayashi, *J. Am. Chem. Soc.* **2001**, *123*, 2438–2439.
- [15] R. Charvet, D. L. Jiang, T. Aida, *Chem. Commun.* **2004**, 2664–2665.
- [16] a) N. C. Maiti, S. Mazumdar, N. Periasamy, *J. Phys. Chem. B* **1998**, *102*, 1528–1538; b) L. A. Lucia, T. Yui, R. Sasai, S. Takagi, K. Takagi, H. Yoshida, D. G. Whitten, H. Inoue, *J. Phys. Chem. B* **2003**, *107*, 3789–3797.
- [17] N. Kobayashi, R. Higashi, B. C. Titeca, F. Lamote, A. Ceulemans, *J. Am. Chem. Soc.* **1999**, *121*, 12018–12028.
- [18] a) H. Harada, K. Nakanishi, *Circular Dichroic Spectroscopy, Exciton Coupling in Organic Stereochemistry*, University Science Books, New York, **1983**; b) N. Kobayashi, *Chem. Commun.* **1998**, 487–488.
- [19] a) J. L. Sessler, J. Jayawickramarajah, A. Gouloumis, G. D. Pantos, T. Torres, D. M. Guldi, *Tetrahedron* **2006**, *62*, 2123–2131; b) K. Adachi, K. Chayama, H. Watarai, *Langmuir* **2006**, *22*, 1630–1639; c) A. W. Snow, in *The Porphyrin Handbook* (Eds.: K. M. Kadish, K. M. Smith, R. Guilard), Elsevier Science, New York, **2003**, p. 129.
- [20] M. Antonietti, S. Förster, *Adv. Mater.* **2003**, *15*, 1323–1333.
- [21] Nanoparticles were obtained when the similar compound H<sub>2</sub>Pc, which lacks the alkyl chains in the binaphthyl units, was fabricated under the same conditions as those used to prepare optically active (R)-1 or (S)-1.
- [22] a) I. Lopez-Salido, D. C. Lim, Y. D. Kim, *Surf. Sci.* **2005**, *588*, 6–18; b) K. Luo, C. T. P. St, D. W. Goodman, *J. Phys. Chem. B* **2000**, *104*, 3050–3057.
- [23] a) J. Janczak, Y. M. Idemori, *Inorg. Chem.* **2002**, *41*, 5059–5065; b) A. S. Gardberg, S. Yang, B. M. Hoffman, J. A. Ibers, *Inorg. Chem.* **2002**, *41*, 1778–1781.
- [24] H. Liu, Y. Liu, M. Liu, C. Chen, F. Xi, *Tetrahedron Lett.* **2001**, *42*, 7083–7086.
- [25] H. Ishitani, M. Ueno, S. Kobayashi, *J. Am. Chem. Soc.* **2000**, *122*, 8180–8186.

Received: May 30, 2008

Published Online: August 19, 2008